



## Dear Author

Here are the proofs of your article.

- You can submit your corrections **online** or by **fax**.
- For **online** submission please insert your corrections in the online correction form. Always indicate the line number to which the correction refers.
- Please return your proof together with the permission to publish confirmation.
- For **fax** submission, please ensure that your corrections are clearly legible. Use a fine black pen and write the correction in the margin, not too close to the edge of the page.
- Remember to note the journal title, article number, and your name when sending your response via e-mail, fax or regular mail.
- **Check** the metadata sheet to make sure that the header information, especially author names and the corresponding affiliations are correctly shown.
- **Check** the questions that may have arisen during copy editing and insert your answers/corrections.
- **Check** that the text is complete and that all figures, tables and their legends are included. Also check the accuracy of special characters, equations, and electronic supplementary material if applicable. If necessary refer to the *Edited manuscript*.
- The publication of inaccurate data such as dosages and units can have serious consequences. Please take particular care that all such details are correct.
- Please **do not** make changes that involve only matters of style. We have generally introduced forms that follow the journal's style. Substantial changes in content, e.g., new results, corrected values, title and authorship are not allowed without the approval of the responsible editor. In such a case, please contact the Editorial Office and return his/her consent together with the proof.
- If we do not receive your corrections **within 48 hours**, we will send you a reminder.

### Please note

Your article will be published **Online First** approximately one week after receipt of your corrected proofs. This is the **official first publication** citable with the DOI.

**Further changes are, therefore, not possible.**

After online publication, subscribers (personal/institutional) to this journal will have access to the complete article via the DOI using the URL:

<http://dx.doi.org/10.1007/s00445-019-1331-8>

If you would like to know when your article has been published online, take advantage of our free alert service. For registration and further information, go to:

<http://www.springerlink.com>.

Due to the electronic nature of the procedure, the manuscript and the original figures will only be returned to you on special request. When you return your corrections, please inform us, if you would like to have these documents returned.

The **printed version** will follow in a forthcoming issue.

**Metadata of the article that will be visualized in OnlineFirst**

|    |                          |   |  |
|----|--------------------------|---|--|
| 1  | Article Title            | <b>The crater lake of Ilamatepec (Santa Ana) volcano, El Salvador: insights into lake gas composition and implications for monitoring</b>                 |  |
| 2  | Article Sub- Title       |   |  |
| 3  | Article Copyright - Year | <b>International Association of Volcanology &amp; Chemistry of the Earth's Interior 2019</b><br><b>(This will be the copyright line in the final PDF)</b> |  |
| 4  | Journal Name             | Bulletin of Volcanology   |  |
| 5  |                          | Family Name   | <b>Aiuppa</b>  |
| 6  |                          | Particle  |  |
| 7  |                          | Given Name  | <b>Alessandro</b>  |
| 8  | Corresponding Author     | Suffix  |  |
| 9  |                          | Organization  | Università di Palermo  |
| 10 |                          | Division  | Dipartimento DiSTeM  |
| 11 |                          | Address   | Palermo, Italy   |
| 12 |                          | e-mail  | alessandro.aiuppa@unipa.it   |
| 13 |                          | Family Name   | <b>Hasselle</b>  |
| 14 |                          | Particle  |  |
| 15 |                          | Given Name  | <b>Nathalie</b>  |
| 16 |                          | Suffix  |  |
| 17 | Author                   | Organization  | Università di Palermo  |
| 18 |                          | Division  | Dipartimento DiSTeM  |
| 19 |                          | Address   | Palermo, Italy   |
| 20 |                          | e-mail  |  |
| 21 |                          | Family Name   | <b>Montalvo</b>  |
| 22 |                          | Particle  |  |
| 23 |                          | Given Name  | <b>Francisco</b>   |
| 24 |                          | Suffix  |  |
| 25 | Author                   | Organization  | Istituto Nazionale di Geofisica e Vulcanologia, Sezione di Bologna |
| 26 |                          | Division  |  |
| 27 |                          | Address   | Bologna, Italy   |
| 28 |                          | e-mail  |  |
| 29 | Author                   | Family Name   | <b>Rouwet</b>  |

|    |        |              |  |
|----|--------|--------------|--|
| 30 |        | Particle     |  |
| 31 |        | Given Name   | <b>Dmitri</b>  |
| 32 |        | Suffix       |  |
| 33 |        | Organization | MARN   |
| 34 |        | Division     | Dirección del Observatorio Ambiental                               |
| 35 |        | Address      | San Salvador, El Salvador  |
| 36 |        | e-mail       |  |
| 37 |        | Family Name  | <b>Battaglia</b>   |
| 38 |        | Particle     |  |
| 39 |        | Given Name   | <b>Angelo</b>  |
| 40 |        | Suffix       |  |
| 41 | Author | Organization | Università di Palermo  |
| 42 |        | Division     | Dipartimento DiSTeM  |
| 43 |        | Address      | Palermo, Italy   |
| 44 |        | e-mail       |  |
| 45 |        | Family Name  | <b>Bitetto</b>   |
| 46 |        | Particle     |  |
| 47 |        | Given Name   | <b>Marcello</b>  |
| 48 |        | Suffix       |  |
| 49 | Author | Organization | Università di Palermo  |
| 50 |        | Division     | Dipartimento DiSTeM  |
| 51 |        | Address      | Palermo, Italy   |
| 52 |        | e-mail       |  |
| 53 |        | Family Name  | <b>Escobar</b>   |
| 54 |        | Particle     |  |
| 55 |        | Given Name   | <b>Demetrio</b>  |
| 56 |        | Suffix       |  |
| 57 | Author | Organization | Istituto Nazionale di Geofisica e Vulcanologia, Sezione di Bologna |
| 58 |        | Division     |  |
| 59 |        | Address      | Bologna, Italy   |
| 60 |        | e-mail       |  |
| 61 |        | Family Name  | <b>Gutiérrez</b>   |
| 62 |        | Particle     |  |
| 63 | Author | Given Name   | <b>Eduardo</b>   |
| 64 |        | Suffix       |  |
| 65 |        | Organization | Istituto Nazionale di Geofisica e Vulcanologia, Sezione di Bologna |

|     |        |              |  |
|-----|--------|--------------|--|
| 66  |        | Division     |  |
| 67  |        | Address      | Bologna, Italy   |
| 68  |        | e-mail       |  |
| 69  |        | Family Name  | <b>Rivera</b>  |
| 70  |        | Particle     |  |
| 71  |        | Given Name   | <b>Jacqueline</b>  |
| 72  |        | Suffix       |  |
| 73  | Author | Organization | Istituto Nazionale di Geofisica e Vulcanologia, Sezione di Bologna |
| 74  |        | Division     |  |
| 75  |        | Address      | Bologna, Italy   |
| 76  |        | e-mail       |  |
| 77  |        | Family Name  | <b>Villalobos</b>  |
| 78  |        | Particle     |  |
| 79  |        | Given Name   | <b>Ana Mirian</b>  |
| 80  |        | Suffix       |  |
| 81  | Author | Organization | Istituto Nazionale di Geofisica e Vulcanologia, Sezione di Bologna |
| 82  |        | Division     |  |
| 83  |        | Address      | Bologna, Italy   |
| 84  |        | e-mail       |  |
| 85  |        | Family Name  | <b>Cioni</b>   |
| 86  |        | Particle     |  |
| 87  |        | Given Name   | <b>R.</b>  |
| 88  |        | Suffix       |  |
| 89  | Author | Organization | Università di Firenze  |
| 90  |        | Division     | Dipartimento di Scienze della Terra                                |
| 91  |        | Address      | Florence, Italy  |
| 92  |        | e-mail       |  |
| 93  |        | Family Name  | <b>Moor</b>  |
| 94  |        | Particle     | <b>de</b>  |
| 95  |        | Given Name   | <b>J. Maarten</b>  |
| 96  |        | Suffix       |  |
| 97  | Author | Organization | UNA-OVSICORI   |
| 98  |        | Division     |  |
| 99  |        | Address      | Heredia, Costa Rica  |
| 100 |        | e-mail       |  |
| 101 | Author | Family Name  | <b>Fischer</b>   |

|     |                             |   |
|-----|-----------------------------|---|
| 102 |                             | Particle  |
| 103 |                             | Given Name <b>Tobias P.</b>   |
| 104 |                             | Suffix  |
| 105 |                             | Organization      University of New Mexico  |
| 106 |                             | Division  |
| 107 |                             | Address            Albuquerque, USA   |
| 108 |                             | e-mail  |
| 109 |                             | Received            24 June 2019  |
| 110 | Schedule                    | Revised   |
| 111 |                             | Accepted            19 October 2019   |
| 112 | Abstract                    | <p>We here present the first chemical characterization of the volcanic gas plume issuing from the Santa Ana crater lake, a hyper-acidic crater lake (pH of - 0.2 to 2.5) in north-western El Salvador. Our results, obtained during regular surveys in 2017 and 2018 using a Multi-GAS instrument, demonstrate a hydrous gas composition (<math>H_2O/SO_2</math> ratios from 32 to 205) and <math>SO_2</math> as the main sulfur species (<math>H_2S/SO_2 = 0.03-0.1</math>). We also find that gas composition evolved during our investigated period, with the <math>CO_2/SO_2</math> ratio decreasing by one order of magnitude from March 2017 (<math>37.2 \pm 9.7</math>) to November 2018 (<math>&lt; 3</math>). This compositional evolution toward more magmatic (<math>SO_2</math>-rich) compositions is interpreted in the context of the long-term evolution of the volcano following its 2005 and 2007 eruptions. We find that, in spite of reduced (background-level) seismicity, the magmatic gas supply into the lake was one order of magnitude higher in March 2017 (total volatile flux: 20,200–30,200 t/day) than in the following periods (total volatile flux: 900–10,167 t/day). We propose that the elevated magmatic/hydrothermal transport in March 2017, combined with a 15% reduction in precipitation, caused the volume of the lake to decrease, ultimately reducing its sulfur absorbing and scrubbing capacity, and hence causing the gas plume <math>CO_2/SO_2</math> ratio to decrease. The recently observed increases in temperature, acidity, and salinity of the lake are consistent with this hypothesis. We conclude that the installation of a continuous, fully-automated Multi-GAS is highly desirable to monitor any future change in lake plume chemistry, and hence the level of degassing activity.</p> |
| 113 | Keywords separated by ' - ' | Santa Ana volcano - Crater lakes - Volcanic gas plumes - Multi-GAS - Gas scrubbing - $CO_2/SO_2$ ratio - Wet volcano  |
| 114 | Foot note information       | <p>Editorial responsibility: P. Allard</p> <p>The online version of this article (<a href="https://doi.org/10.1007/s00445-019-1331-8">https://doi.org/10.1007/s00445-019-1331-8</a>) contains supplementary material, which is available to authorized users.</p>   |

## Electronic supplementary material

### Table S1

Summary of all derived (molar) gas ratios in the Santa Ana crater lake plume.

# AUTHOR'S PROOF!

For each ratio, the correlation coefficient of the best-fit regression line is indicated ( $R^2$ ). SO<sub>2</sub> MAX is the peak SO<sub>2</sub> concentration measured in each measurement interval where a ratio was calculated. (XLS 65 kb)

# The crater lake of Ilamatepec (Santa Ana) volcano, El Salvador: insights into lake gas composition and implications for monitoring

Nathalie Hasselle<sup>1</sup> · Francisco Montalvo<sup>2</sup> · Dmitri Rouwet<sup>3</sup> · Angelo Battaglia<sup>1</sup> · Marcello Bitetto<sup>1</sup> · Demetrio Escobar<sup>2</sup> · Eduardo Gutiérrez<sup>2</sup> · Jacqueline Rivera<sup>2</sup> · Ana Mirian Villalobos<sup>2</sup> · R. Cioni<sup>4</sup> · J. Maarten de Moor<sup>5</sup> · Tobias P. Fischer<sup>6</sup> · Alessandro Aiuppa<sup>1</sup>

Received: 24 June 2019 / Accepted: 19 October 2019

© International Association of Volcanology & Chemistry of the Earth's Interior 2019

## Abstract

We here present the first chemical characterization of the volcanic gas plume issuing from the Santa Ana crater lake, a hyperacidic crater lake (pH of −0.2 to 2.5) in north-western El Salvador. Our results, obtained during regular surveys in 2017 and 2018 using a Multi-GAS instrument, demonstrate a hydrous gas composition ( $H_2O/SO_2$  ratios from 32 to 205) and  $SO_2$  as the main sulfur species ( $H_2S/SO_2 = 0.03–0.1$ ). We also find that gas composition evolved during our investigated period, with the  $CO_2/SO_2$  ratio decreasing by one order of magnitude from March 2017 ( $37.2 \pm 9.7$ ) to November 2018 ( $< 3$ ). This compositional evolution toward more magmatic ( $SO_2$ -rich) compositions is interpreted in the context of the long-term evolution of the volcano following its 2005 and 2007 eruptions. We find that, in spite of reduced (background-level) seismicity, the magmatic gas supply into the lake was one order of magnitude higher in March 2017 (total volatile flux: 20,200–30,200 t/day) than in the following periods (total volatile flux: 900–10,167 t/day). We propose that the elevated magmatic/hydrothermal transport in March 2017, combined with a 15% reduction in precipitation, caused the volume of the lake to decrease, ultimately reducing its sulfur absorbing and scrubbing capacity, and hence causing the gas plume  $CO_2/SO_2$  ratio to decrease. The recently observed increases in temperature, acidity, and salinity of the lake are consistent with this hypothesis. We conclude that the installation of a continuous, fully-automated Multi-GAS is highly desirable to monitor any future change in lake plume chemistry, and hence the level of degassing activity.

**Keywords** Santa Ana volcano · Crater lakes · Volcanic gas plumes · Multi-GAS · Gas scrubbing ·  $CO_2/SO_2$  ratio · Wet volcano

Editorial responsibility: P. Allard

**Electronic supplementary material** The online version of this article (<https://doi.org/10.1007/s00445-019-1331-8>) contains supplementary material, which is available to authorized users.

✉ Alessandro Aiuppa  
alessandro.aiuppa@unipa.it

<sup>1</sup> Dipartimento DiSTeM, Università di Palermo, Palermo, Italy

<sup>2</sup> Istituto Nazionale di Geofisica e Vulcanologia, Sezione di Bologna, Bologna, Italy

<sup>3</sup> Dirección del Observatorio Ambiental, MARN, San Salvador, El Salvador

<sup>4</sup> Dipartimento di Scienze della Terra, Università di Firenze, Florence, Italy

<sup>5</sup> UNA-OVSICORI, Heredia, Costa Rica

<sup>6</sup> University of New Mexico, Albuquerque, USA

## Introduction

The term wet volcano was introduced by Caudron et al. (2015) and is used to define a volcanic system characterized by the presence of an active voluminous magmatic-hydrothermal system. At such systems, the physical-chemical properties of crater lakes are key to volcanic activity monitoring (e.g., Rowe et al. 1992; Takano et al. 1994; Ohba et al. 2008; Christenson et al. 2010, 2015; Shinohara et al. 2015; Agosto and Varekamp 2016; de Moor et al. 2016a, 2019; Caudron et al. 2017). Temporal variations in the lake's physical-chemical state are thought to result from time-changing rates of heat and fluid supply from the underlying magmatic-hydrothermal system (e.g., Rowe et al. 1992; Christenson 2000; Ohba et al. 2008). However, Rouwet et al. (2016) has recently postulated that classic monitoring techniques, involving analysis of dissolved components in hyper-acidic crater lakes, are often of too low a temporal resolution to capture

47 precursory signals to phreatic eruptions, the main hazard related to peak-activity crater lakes (e.g., Christenson et al. 2010; de Moor et al. 2016a, 2019). This observation has motivated further work to provide higher temporal resolution time series to track long- and short-term changes at crater lakes, to identify the parameters that need to be measured, and the processes they can be used to track.

54 The magmatic gas species usually monitored in fumaroles and plumes of open-vent volcanoes (Fischer and Chiodini 2015) can also be detected in the gas plumes released by hyper-acidic lakes. For hyper-acidic lake conditions, CO<sub>2</sub> is not absorbed into lake water, but SO<sub>2</sub> variably reacts with lake water to form H<sub>2</sub>SO<sub>4</sub> (e.g., Tamburello et al. 2015; de Moor et al. 2016a, 2019; Gunawan et al. 2016), and HCl degassing accelerates if pH < 0 conditions are met (Capaccioni et al. 2017). The Multi-GAS instrument (Aiuppa et al. 2005a; Shinohara 2005), while traditionally used to monitor volcanic gas composition at “dry volcanoes” (e.g., Aiuppa et al. 2009, 2018; de Moor et al. 2016b), has recently proven to be useful in measuring gas plumes from crater lakes (Shinohara et al. 2015; Tamburello et al. 2015; Gunawan et al. 2016; Hasselle et al. 2018) and in detecting precursory changes to phreatic eruptions (de Moor et al. 2016a, 2019). High-frequency, continuous observations of gas compositions discharging from lakes can be of paramount importance in monitoring volcanic activity and in forecasting phreatic/phreatomagmatic eruptions (Stix and de Moor 2018; Battaglia et al. 2019).

76 Here, we characterize for the first time the composition of the lake gas plume released by Santa Ana crater lake (March 2017–November 2018). We interpret the temporal changes observed in tandem with lake level

80 variations, SO<sub>2</sub> flux record, and seismicity, in an attempt to derive constraints on the current activity state and to speculate on the potential changes that might herald future reactivation of this restless volcano.

### Geological and volcanological settings

84 Ilamatepec or Santa Ana volcano (13° 51' N, 89° 37.5' W; 2381 m asl) is located in western El Salvador (Fig. 1) and is surrounded by two highly populated cities, Santa Ana (pop. 522,000) and Sonsonate (pop. 420,000), both lying within a radius of 25 km from the volcano (Pullinger 1998; Colvin 2008). It is one of the most active volcanoes in El Salvador, with 13 VEI 2–3 eruptions reported since AD 1500 (Mooser et al. 1958; GVP 2018), mostly phreatic to phreatomagmatic in nature (Pullinger 1998). The last magmatic eruption occurred on October 1, 2005 (Scolamacchia et al. 2010) and was followed by small phreatic eruptions on March 15 and April 27, 2007. The youngest of the current four summit craters (0.5-km diameter) has hosted a small hyper-acidic crater lake (Bernard et al. 2004; Colvin 2008; Colvin et al. 2013) since 1904 (Carr and Pontier 1981).

101 The Santa Ana-Izalco-Coatepeque volcanic complex (< 200 ka; Pullinger 1998) includes two stratovolcanoes (Santa Ana and Izalco), the Coatepeque caldera (that is filled with a lake, Cabassi et al. 2019), and many parasitic cones, cinder cones, and explosion craters (Fig. 1; Pullinger 1998). The complex is part of the Central American Volcanic Arc, which results from subduction of the Cocos Plate below the Caribbean Plate (Carr 1984; DeMets et al. 1990).

**Fig. 1** Google Earth image (Image © 2019 Maxar Technologies) of the Santa Ana volcano and its surroundings. The location of the DOAS and seismic stations run by MARN are indicated. Inset: location of Santa Ana volcano in Central America





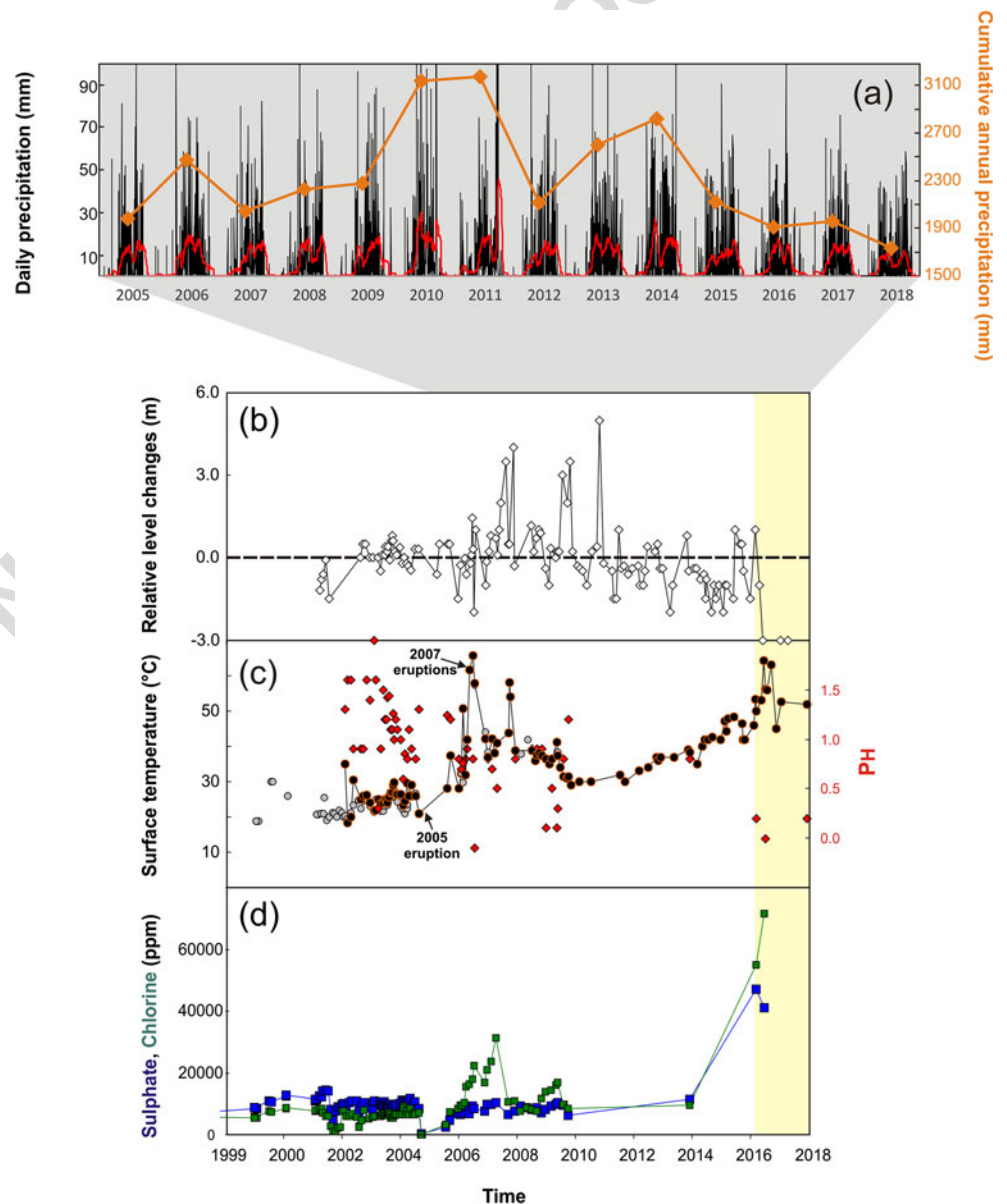
109 **Temporal evolution of the crater lake**

110 A large and permanent hydrothermal system beneath the volcano is implied by the many phreatic to phreatomagmatic  
 111 eruptions of Santa Ana in the last thousand years (Pullinger  
 112 1998; Bernard et al. 2004). The hydrothermal system, topped  
 113 by the hyper-acidic crater lake, manifests as hot springs along  
 114 the lake shore, lake gas bubbling, and fumarolic emissions  
 115 west of the lake. In 2000–2002, the lake floor was bowl-  
 116 shaped, with a diameter of 200 m and a maximum depth of  
 117 27 m (Bernard et al. 2004). Along the shoreline, bubbling hot  
 118 springs were observed ( $T \sim 80^\circ\text{C}$ ; Bernard et al. 2004). Prior to  
 119 the October 2005 eruption, high-temperature fumaroles  
 120 discharged vigorously although showing a marked tempera-  
 121 ture decline between 2002 and 2003 (being  $532^\circ\text{C}$  in January  
 122

2000,  $875^\circ\text{C}$  in June 2002,  $264^\circ\text{C}$  in December 2003,  $360^\circ\text{C}$   
 in January 2004; Bernard et al. 2004; Scolamacchia et al.  
 2010; SNET Monthly Report). The 2005 and 2007 eruptions  
 drastically modified lake geometry, temperature, and  
 water chemistry, possibly due to changes in rate and com-  
 position of the volcanic gas input (Colvin 2008; Colvin  
 et al. 2013; Laiolo et al. 2017) (Fig. 2). The discharge rate  
 and temperature of the fumaroles also decreased (to  $< 100^\circ\text{C}$ ).  
 However, the period 2010–2014 was poorly docu-  
 mented, inhibiting detailed evaluation of the activity of  
 Santa Ana crater lake (Fig. 2).

Colvin (2008) proposed a physical model of the Santa Ana  
 magmatic-hydrothermal system. According to Colvin (2008),  
 a shallow degassing magma body (3–7 km depth, Carr and  
 Pontier 1981; Halsor and Rose 1988) was overlain by a single-

**Fig. 2** Temporal variations in crater lake level, chemico-physical parameters and chemistry, 1999–2018 (the yellow-colored band identifies the temporal window covered by our Multi-GAS observations). **a** Daily precipitations (in mm) in the Santa Ana area (black line, left axis; the red solid line is a 30-day mobile average). The cumulative yearly precipitations. **b** Changes in lake level, in meters, expressed relative to a fixed benchmark position in the inner crater walls. **c** Temporal changes in lake surface temperature (left scale, gray circles, Bernard et al. 2004; Scolamacchia et al. 2010; black circles, MARN monitoring database) and pH (right scale; red diamonds). **d** Dissolved  $\text{SO}_4$  and Cl concentrations in the lake water are also shown (orange diamonds, right y-scale). Data from MARN monitoring database



138 phase vapor zone and acid-sulfate-chloride hot springs (before  
 139 the 2005 eruption; Bernard et al. 2004). This vapor zone  
 140 would be separated from a shallower (near-surface) two-  
 141 phase (liquid + gas) region by a low-permeability mineral seal  
 142 (Pullinger 1998; Bernard et al. 2004). The fumarolic field,  
 Q4 143 present since at least the 1950s (Meyer-Abich 1956; Bernard  
 144 et al. 2004), was ruptured during the 2005 eruption (Colvin  
 145 et al. 2013). After the eruption, this part of the crater was  
 146 flooded but the presence of sub-lacustrine fumaroles is  
 147 highlighted by strong bubbling driving a vigorous convection  
 148 cell at the lake surface. This was still visible in 2018.

149 Periodical changes in activity are common in the recent  
 150 history of Santa Ana crater lake. High activity levels were  
 151 reported in 1920 and July 1992 (Gutiérrez and Escobar  
 152 1994; Bernard et al. 2004). More recently, low-level activity  
 153 periods (January–May 2000 and February 2002–June 2004)  
 154 alternated with high activity periods (May 2000–February  
 155 2002 and June 2004–August 2005) and finally culminated in  
 156 eruption on October 1, 2005 (Colvin 2008). Before (October  
 157 2005–March 2007) and after (May 2007–December 2007) the  
 158 March–April 2007 phreatic eruptions, Colvin (2008) reported  
 159 a high level of activity.

160 The recent evolution of the lake system, illustrated in Fig.  
 161 2, is characterized thanks to monitoring results provided by  
 162 MARN (Ministerio de Medio Ambiente e Recursos  
 163 Naturales), the Salvadoran environmental and natural re-  
 164 sources research office. MARN regularly monitors fumarole  
 165 temperature, lake water temperature, and pH, as well as me-  
 166 teoric precipitation at the Los Naranjos station (approximately  
 167 3 km NNW of Santa Ana crater lake) (Fig. 2a). Variations in  
 168 crater lake level (Fig. 2b) are also assessed by MARN com-  
 169 paring the lake level from photographs taken at several dates  
 170 with the lake level on a scaled reference photograph.  
 171 According to MARN database and previous literature infor-  
 172 mation (see figure caption for details), the pH of the lake water  
 173 (Fig. 2c) showed strong fluctuations, between 2 and 0.5, be-  
 174 fore the 2005 and 2007 eruptions; after the March–April 2007  
 175 phreatic eruptions, the lake water pH dropped to  $-0.2$ , the  
 176 lowest pH measured so far. A sudden temperature rise of  $10$   
 177  $^{\circ}\text{C}$  occurred prior to the 2007 eruptions (Fig. 2c). Afterwards,  
 178 the lake level oscillated considerably, but mostly rose after the  
 179 2007 eruption and until 2010. By mid-2010, lake water tem-  
 180 perature had returned to pre-phreatic lake temperatures of  $28$ –  
 181  $32$   $^{\circ}\text{C}$ . From 2011, two main periods of lake level drop were  
 182 observed in 2014–2015 and in June 2017 to January 2018.  
 183 Since February 2011, the lake water temperature started a  
 184 steady increasing trend, with a peak temperature registered  
 185 in June 2017, yet below the pre-phreatic eruptive temperature  
 186 of  $65.6$   $^{\circ}\text{C}$ . The most recent pH values are near zero, among  
 187 the highest on record. Sulfate and chloride concentrations in  
 188 the crater lake water both peaked in 2017, at respectively  
 189  $41,000$ – $47,000$  mg/L and  $54,000$ – $71,000$  mg/L (Fig. 2d). No  
 190 data on water chemistry are available for 2018.

**Methods**

191 We investigated the composition of gases emitted from the  
 192 surface of Santa Ana crater lake. Gas compositions were mea-  
 193 sured in situ by Multi-GAS (multicomponent gas analyser  
 194 system) (Aiuppa et al. 2005a; Shinohara 2005). We used a  
 195 compact sensor unit containing a non-dispersive infrared  
 196Q5 (NDIR) spectrometer (for  $\text{CO}_2$ ; range =  $0$ – $3000$  ppm); three  
 197 electrochemical gas sensors for  $\text{H}_2\text{S}$  (range =  $0$ – $100$  ppm),  
 198  $\text{SO}_2$  (range =  $0$ – $200$  ppm), and  $\text{H}_2$  (range =  $0$ – $200$  ppm);  
 199 and a relative humidity sensor (range =  $0$ – $100\%$ ) for indirectly  
 200 measuring  $\text{H}_2\text{O}$ . 201

202 An explorative Multi-GAS survey was conducted at Santa  
 203 Ana in March 2017 to investigate the composition of the lake  
 204 gas plume for the first time. Measurements were obtained  
 205 using a mobile Multi-GAS from three distinct sites in the  
 206 crater area, located at different distances from the lake (Fig.  
 207 3): (i) on the S and SW outer crater rims,  $> 400$  m from the  
 208 lake; (ii) on the plateau,  $\sim 200$  m NNE from the lake; and (iii)  
 209 on the eastern lake shore. The same operations, at the same  
 210 measurement sites, were repeated in June 2017, and a contin-  
 211 uously recording Multi-GAS (measuring at  $0.5$  Hz rate in  $4$   
 212 daily measurement cycles of  $30$  min each) was run on the  
 213 plateau site between June 5 and 13 (Fig. 3). Based on the  
 214 results of these initial surveys, the plateau site (Fig. 3) was  
 215 selected as the best location for deployment of a semi-  
 216 permanent station, owing to relatively safe access compared  
 217 to the lake shore and denser plume conditions compared to the  
 218 outer rim. This semi-permanent station operated in April 2018  
 219 for 3 days, while punctual measurements for periods of  $\sim 2$  to  
 220  $3$  h were also performed at the same site on May 3 and  
 221 June 28, 2018. In November 2018, measurements were taken  
 222 at both the plateau and the lake shore. Analytical data are  
 223 summarized in Table S1. During the periods of observation,  
 224 only a few low-temperature weakly degassing fumaroles (and  
 225 a few hot springs) were visible, mostly on the SW shore and  
 226 on the inner crater slope.

227 During our measurement period, both seismicity and  
 228  $\text{SO}_2$  fluxes remained at background levels (Fig. 4), at least  
 229 relative to records obtained during the 2005 eruptive un-  
 230 rest (Olmos et al. 2007). Seismicity was registered at the  
 231 MARN seismic station located at San Blas,  $1$  km SE from  
 232 the crater (Fig. 1). The  $\text{SO}_2$  fluxes were measured with the  
 233 permanent DOAS instrument of the NOVAC network  
 234 (Galle et al. 2010), installed at  $6$  km SW from the crater  
 235 (Fig. 1) and elaborated by the MARN monitoring service.  
 236 During our specific Multi-GAS measurements in 2017–  
 237 2018, the  $\text{SO}_2$  flux varied from  $41$  and  $329$  t/day and  
 238 was slightly higher in 2017 (mean  $165 \pm 140$  t/day) than  
 239Q6 in 2018 (mean  $144 \pm 77$  t/day) (Table 1). Considering the  
 240 absence of high-temperature fumaroles during the studied  
 241 period, we consider the degassing crater lake as the ex-  
 242 clusive source of the  $\text{SO}_2$  detected by the DOAS.

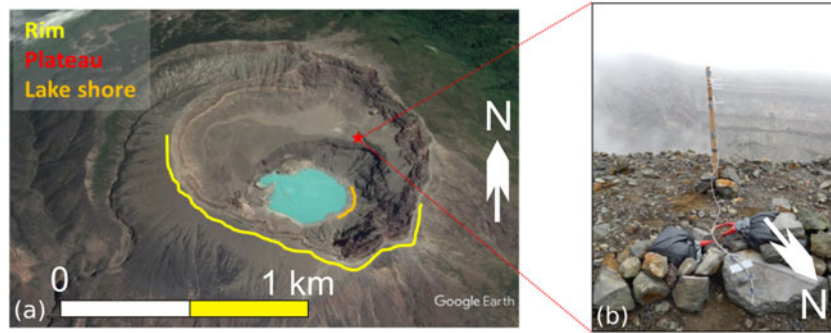


**Fig. 3** a Google Earth image of Santa Ana volcano (Image © 2019 Maxar Technologies) with the location and tracks of Multi-GAS measurements in March 2017. The yellow and orange tracks correspond to measurements carried out by walking along the rim and

the lake shore, respectively. The red star is the plateau measurement site. It is also the location where the a semi-permanent Multi-GAS was installed in June 2017 and in 2018 (b).

243 **Results**

244 Examples of Multi-GAS acquisitions at the three sites (rim,  
 245 plateau, and lake shore), taken in the explorative March 2017  
 246 campaign, are given in Fig. 5. At the crater outer rim, in March  
 247 and June 2017, we detected low amounts of SO<sub>2</sub> (~ 1 ppm)  
 248 and H<sub>2</sub>O (~ 1000s ppm above atmospheric background) (Fig.  
 249 5). H<sub>2</sub>S concentrations were very low (~ 0.1–0.4 ppm) and

poorly correlated with SO<sub>2</sub> peaks, and the volcanic plume was 250  
 typically too diluted for a volcanic CO<sub>2</sub> signal to be resolved 251  
 over the atmospheric background (Fig. 5a). At the plateau and 252  
 the lake shore, all the target volcanic gases (CO<sub>2</sub>, SO<sub>2</sub>, H<sub>2</sub>, and 253  
 H<sub>2</sub>O) were detectable in the plume at concentrations higher 254  
 than 1 ppm (see examples shown in Fig. 5b, c). At the plateau, 255  
 gas concentrations varied considerably over time. In the 256  
 acquisition example of Fig. 5b, SO<sub>2</sub>, CO<sub>2</sub>, H<sub>2</sub>, H<sub>2</sub>O, and H<sub>2</sub>S 257

**Fig. 4** 2005–2018 time series of the seismic activity giving a number of volcanic events, V; b number of volcano-tectonic earthquakes, VT; c Real-time Seismic-Amplitude Measurement (RSAM); and d SO<sub>2</sub> flux at Santa Ana

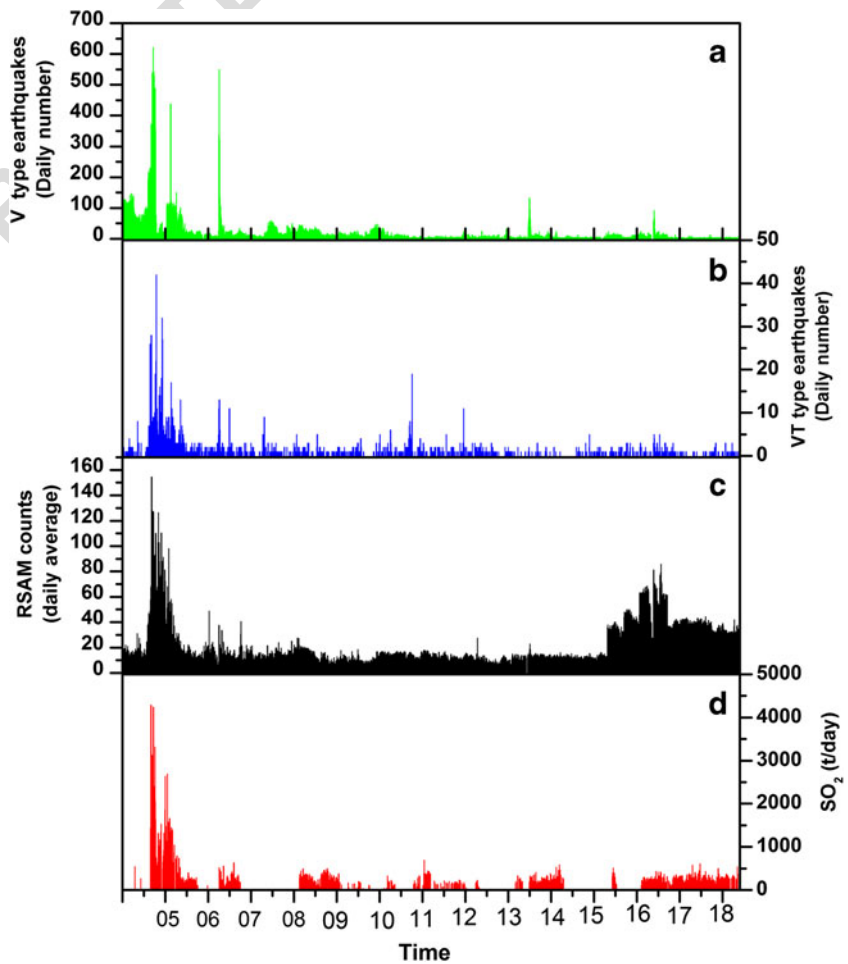


**Table 1** Daily averaged gas ratios (molar) at the plateau and lake shore, calculated by averaging all the ratios from Table S1 where peak SO<sub>2</sub> concentrations is higher than 7 ppm (filtered dataset). The gas fluxes (in tons/day) were calculated by scaling the daily mean gas ratios to the daily averaged SO<sub>2</sub> fluxes from the MARN DOAS station. 1σ is the standard deviation

| t1.2  | Date       | Location | Peak SO <sub>2</sub> | CO <sub>2</sub> /SO <sub>2</sub> | 1 SD | H <sub>2</sub> /SO <sub>2</sub> | 1 SD | H <sub>2</sub> O/SO <sub>2</sub> | 1 SD | H <sub>2</sub> S/SO <sub>2</sub> | 1 SD | SO <sub>2</sub> flux | 1 SD | CO <sub>2</sub> flux | 1 SD | H <sub>2</sub> flux | 1 SD | H <sub>2</sub> O flux | 1 SD | H <sub>2</sub> S flux | 1 SD | TV flux | 1 SD   |  |
|-------|------------|----------|----------------------|----------------------------------|------|---------------------------------|------|----------------------------------|------|----------------------------------|------|----------------------|------|----------------------|------|---------------------|------|-----------------------|------|-----------------------|------|---------|--------|--|
| t1.3  | 07/03/2017 | Shore    | 16.5                 | 31                               | 13.7 | 0.42                            | 0.11 | 0.27                             | 0.06 | 0.03                             | 0.03 | 240                  | 96   | 5112                 | 3049 | 3.1                 | 1.5  |                       |      |                       |      |         |        |  |
| t1.4  | 07/03/2017 | Plateau  | 8.2                  | 37.2                             | 9.7  | 2.39                            | 0.27 | 205                              | 14   | 0.03                             | 0.02 | 240                  | 96   | 6135                 | 2931 | 18                  | 7.5  | 13.825                | 5615 |                       |      | 20,217  | 8649   |  |
| t1.5  | 08/03/2017 | Shore    | 26.6                 | 54.5                             | 24.9 | 0.54                            | 0.06 | 190                              | 11   | 0.03                             | 0.01 | 329                  | 132  | 12,320               | 7486 | 5.5                 | 2.3  | 17,565                | 7106 | 5.2                   | 2.7  | 30,225  | 14,728 |  |
| t1.6  | 05/06/2017 | Plateau  | 10.3                 | 4.7                              | 1.9  | 0.46                            | 0.31 |                                  |      | 0.03                             | 0.02 | 51                   | 20   | 165                  | 94   | 0.7                 | 0.6  |                       |      | 0.8                   | 0.6  |         |        |  |
| t1.7  | 13/06/2017 | Shore    | 20                   | 5.4                              | 0.1  | 0.06                            | 0.02 | 77.4                             | 3.9  |                                  |      | 41                   | 16   | 152                  | 61   | 0.1                 | 0.04 | 892                   | 360  |                       |      | 1085    | 437    |  |
| t1.8  | 13/06/2017 | Plateau  | 15.6                 | 4.2                              | 1.4  | 0.84                            | 0.75 | 75.8                             | 48.2 | 0.06                             | 0.03 | 41                   | 16   | 118                  | 62   | 1.1                 | 1.1  | 873                   | 657  | 1.3                   | 0.8  | 1035    | 737    |  |
| t1.9  | 06/04/2018 | Plateau  | 14.7                 | 4.1                              | 1.6  | 0.52                            | 0.57 | 177                              | 11   | 0.08                             | 0.02 | 87                   | 35   | 245                  | 137  | 1.4                 | 1.6  | 4327                  | 1753 | 3.7                   | 1.7  | 4664    | 1928   |  |
| t1.10 | 12/04/2018 | Plateau  | 26.7                 | 3.3                              | 1.1  | 0.44                            | 0.27 | 82                               | 34   | 0.1                              | 0.07 | 214                  | 86   | 485                  | 253  | 2.9                 | 2.2  | 4931                  | 2843 | 11                    | 9.2  | 5644    | 3193   |  |
| t1.11 | 13/04/2018 | Plateau  | 24.8                 | 3.2                              | 0.7  | 0.39                            | 0.17 | 62                               | 37   | 0.08                             | 0.07 | 61                   | 24   | 134                  | 61   | 0.7                 | 0.4  | 1063                  | 764  | 2.6                   | 2.5  | 1261    | 853    |  |
| t1.12 | 14/04/2018 | Plateau  | 17.6                 | 3.3                              | 0.5  | 0.44                            | 0.21 | 32                               | 18   |                                  |      | 81                   | 32   | 184                  | 79   | 1.1                 | 0.7  | 728                   | 503  |                       |      | 994     | 615    |  |
| t1.13 | 03/05/2018 | Plateau  | 29.5                 | 2.9                              | 0.8  | 0.39                            | 0.15 | 75                               | 26   |                                  |      | 117                  | 47   | 233                  | 113  | 1.4                 | 0.8  | 2466                  | 1306 |                       |      | 2817    | 1467   |  |
| t1.14 | 28/06/2018 | Plateau  | 25.8                 | 2.4                              | 0.5  | 0.37                            | 0.14 | 107                              | 19   |                                  |      | 231                  | 92   | 381                  | 172  | 2.7                 | 1.5  | 6945                  | 3042 |                       |      | 7560    | 3308   |  |
| t1.15 | 28/11/2018 | Shore    | 41.5                 | 2.7                              | 0.2  |                                 |      | 143                              | 8    | 0.08                             | 0.03 | 236                  | 94   | 438                  | 178  |                     |      | 9483                  | 3834 | 10                    | 5.5  | 10,167  | 4112   |  |
| t1.16 | 28/11/2018 | Plateau  | 25                   | 2.9                              | 0.2  | 0.6                             | 0.1  | 90                               | 25   |                                  |      | 236                  | 94   | 470                  | 191  | 4.4                 | 1.9  | 5968                  | 2909 |                       |      | 6679    | 3196   |  |

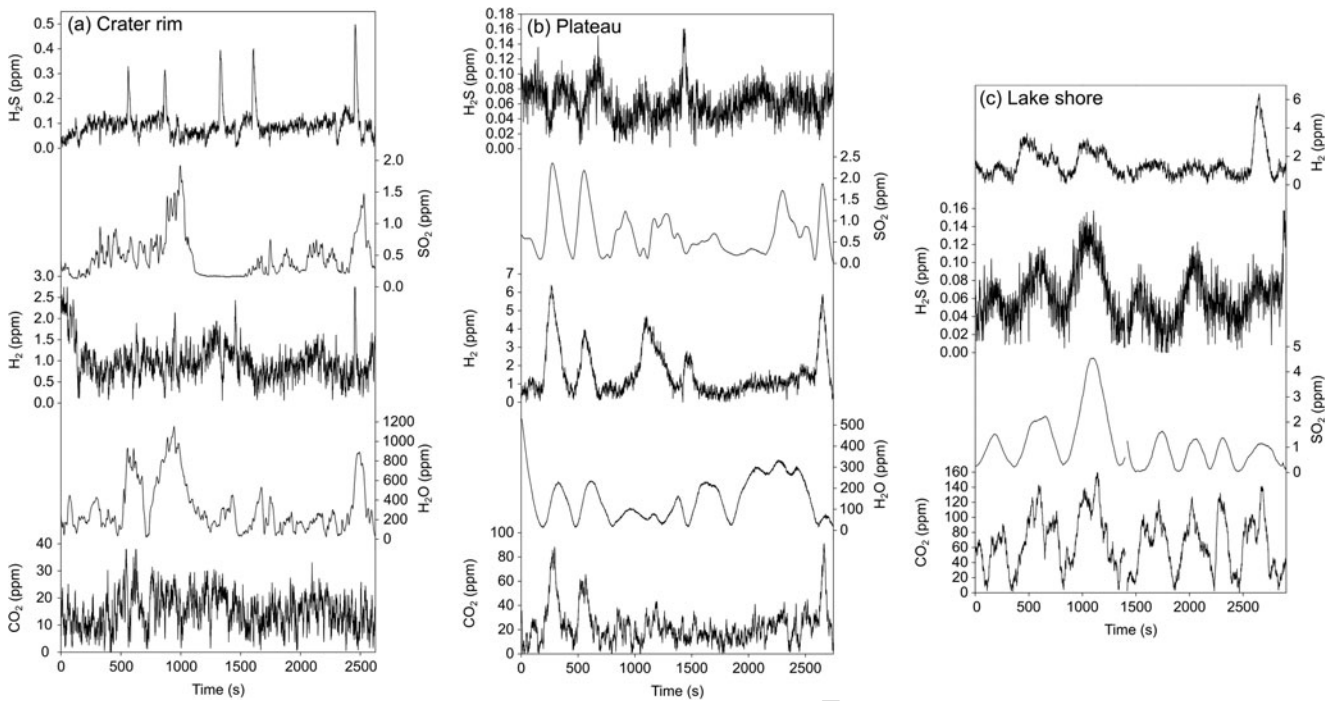


**Fig. 5** Examples of Multi-GAS measurements at the crater rim (a), plateau (b), and lake shore (c) in March 2017

258 concentrations peaked at ~ 2.5, 80, 6, 300, and 0.14 ppm,  
 259 respectively. Higher gas concentrations were observed episodically (in other acquisition windows), with peak concentrations  
 260 of up to ~ 20 ppm for SO<sub>2</sub>, ~ 150 ppm for CO<sub>2</sub> (above the atmospheric background of 403 ppm), ~ 20 ppm for H<sub>2</sub>, ~  
 261 3000 ppm for H<sub>2</sub>O (above background), and ~ 1.3 ppm for H<sub>2</sub>S (see Table S1). Measurements at the lake shore found the  
 262 densest plume conditions (~ 30 ppm for SO<sub>2</sub>) (Table S1). For practicality and safety reasons, the plateau site was selected for  
 263 observations in 2018, except in November when the plateau and the lake shore were both accessed for measurement (Table S1).  
 264

265 The acquired concentration time series were processed  
 266 using the scatter plot technique described by Hasselle et al.  
 267 (2018). To do this, sequences of scatter plots (e.g., Fig. 6) were  
 268

272 built for all sub-intervals where well-correlated concentration  
 273 peaks were observed. Gas ratios were then obtained from the  
 274 gradients of the best-fit regression lines. Gas ratios derived in  
 275 this way are listed in the Appendix or Supplement (Table S1)  
 276 and illustrated in the H<sub>2</sub>/SO<sub>2</sub> vs. CO<sub>2</sub>/SO<sub>2</sub> scatter plot of Fig.  
 277 7. The plot shows that both ratios span more than one order  
 278 of magnitude and define a general compositional trend from  
 279 SO<sub>2</sub>-rich to H<sub>2</sub>-CO<sub>2</sub>-rich compositions. Our results also show  
 280 that, even at the plateau location where a dense gas plume was  
 281 detected, the obtained H<sub>2</sub>/SO<sub>2</sub> ratios and, to a minor extent,  
 282 the CO<sub>2</sub>/SO<sub>2</sub> ratios were anti-correlated with SO<sub>2</sub> concentrations (Fig. 8), as observed elsewhere (e.g., at Masaya; Aiuppa  
 283 et al. 2018). We cannot exclude that the high gas ratios at low  
 284 SO<sub>2</sub> concentrations were (even partially) due to difficulties in  
 285 resolving volcanic H<sub>2</sub> and CO<sub>2</sub> signals over the atmospheric  
 286 backgrounds in dilute plume conditions—if so, the derived  
 287 H<sub>2</sub>/SO<sub>2</sub> and CO<sub>2</sub>/SO<sub>2</sub> ratios would over-estimate the real volcanic  
 288 signatures. Because of this possible concern, we find it  
 289 more prudent to analyze the temporal trends in gas composition  
 290 (Fig. 9) concentrating on the ratios obtained for sub-intervals  
 291 with SO<sub>2</sub> above a 7-ppm concentration threshold where ratios  
 292 become independent of SO<sub>2</sub> concentrations (Fig. 8). The daily  
 293 averaged gas ratios derived from the filtered (> 7 ppmv SO<sub>2</sub>)  
 294 dataset are listed in Table 1.  
 295

296 Our filtered dataset highlights considerable changes in gas  
 297 composition during the investigated period (Table 1 and Fig.  
 298 9). In March 2017, we were only able to obtain CO<sub>2</sub>/SO<sub>2</sub> and  
 299 H<sub>2</sub>/SO<sub>2</sub> ratios at both the plateau and lake shore (Fig. 9 and  
 300 Table 1). The daily averaged CO<sub>2</sub>/SO<sub>2</sub> ratios were similarly  
 301 high at both lake shore (31.0 ± 13.7) and plateau (37.2 ± 9.7).  
 302

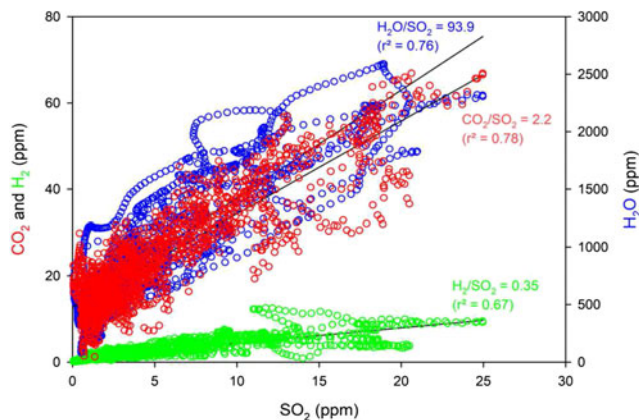
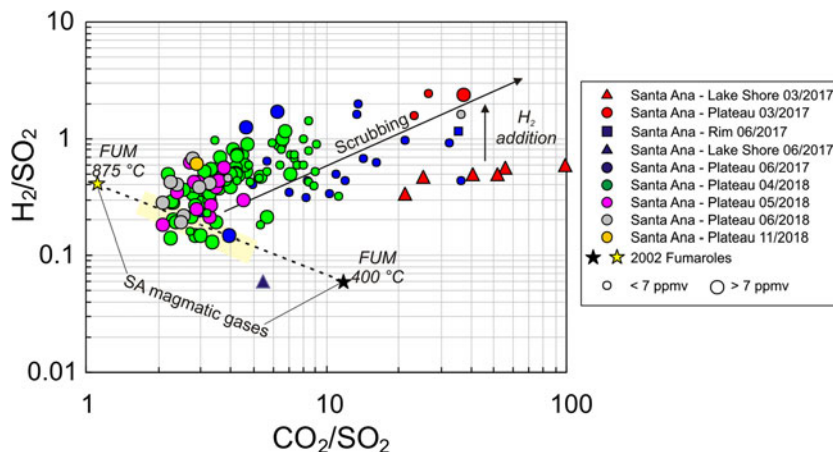


**Fig. 6** Example of gas vs. SO<sub>2</sub> correlation plot in the form of a CO<sub>2</sub>, H<sub>2</sub>, H<sub>2</sub>O vs. SO<sub>2</sub> scatter plot. Data taken at the plateau on June 28, 2018

**Fig. 7**  $H_2/SO_2$  vs.  $CO_2/SO_2$  ratios of Santa Ana lake gas emissions in 2017–2018 (data from Table S1). The compositions of high temperature fumaroles collected in June 2002 are also shown (sampled and analyzed by T.F.). From these, the yellow-colored area represents the inferred hypothetical composition of magmatic gases entering the Santa Ana crater lake in 2017–2018. FUM = fumarole as sampled by T.F.



302 The  $H_2/SO_2$  ratios were  $0.42 \pm 0.11$  at the lake shore and  
 303 higher ( $2.39 \pm 0.27$ ) at the plateau. In June 2017, the  $CO_2/SO_2$   
 304 ratios were drastically lower than in March (see Table 1),  
 305 and again similar at both measurement sites ( $5.4 \pm 0.1$  at the  
 306 lake shore and  $4.2 \pm 1.4$  at the plateau; Fig. 9). The same

contrast in  $H_2/SO_2$  ratios (already seen in March) between 307  
 lake shore ( $0.06 \pm 0.02$ ) and plateau ( $0.46$  to  $0.84 \pm 0.75$ ) 308  
 was observed, but at both sites, a  $H_2$ -poorer ( $SO_2$ -richer) gas 309  
 than in March was detected. The  $H_2S/SO_2$  ratios were similar 310  
 in March and June 2017 ( $0.03$  to  $0.06$ ). The daily averaged 311  
 $H_2O/SO_2$  ratios were of 190 to 205 in March 2017 and of 75.8 312  
 to 77.4 in June (Table 1). 313

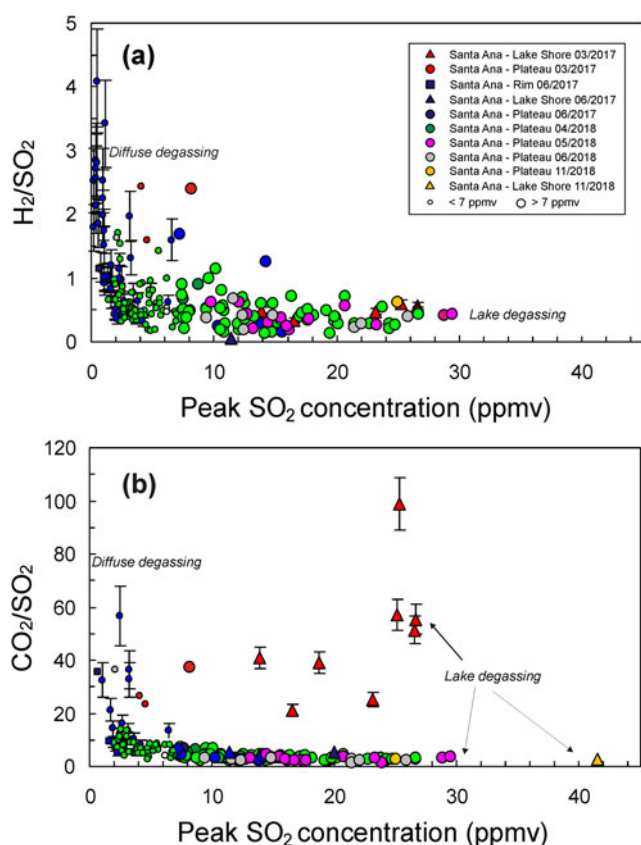


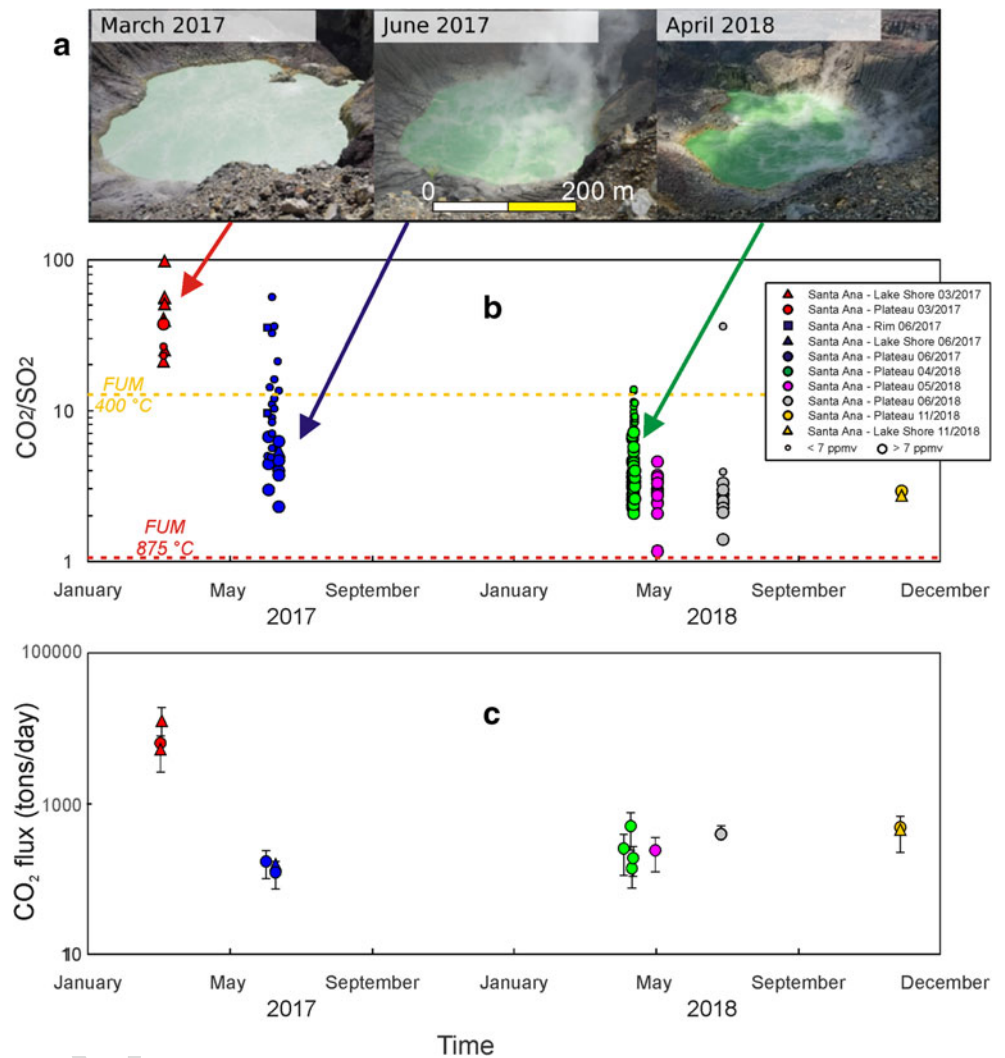
**Fig. 8** Scatter plots of derived **a**  $H_2/SO_2$  and **b**  $CO_2/SO_2$  ratios vs. the peak  $SO_2$  concentration in each integration interval (data from Table S1). At low ( $< 7$  ppmv  $SO_2$ , small symbols) gas concentrations, the derived ratios are negatively correlated with  $SO_2$  (taken as a proxy of plume density). At higher ( $> 7$  ppm of  $SO_2$ , large symbols), gas ratios are independent on concentrations and are thus well representative of lake degassing only. The vertical error bars illustrate errors in the derived ratios (shown for a few selected data point only for clarity)

A further decrease in  $CO_2/SO_2$  ratios was observed at the 314  
 plateau in April, May, June, and November 2018, when the daily 315  
 averaged ratio ranged between  $4.1 \pm 1.6$  (April) and  $2.4 \pm 0.5$  316  
 (June) (Table 1; Fig. 9). The  $H_2/SO_2$  ratios in May–June 2018 317  
 were also the lowest (daily averages from  $0.37 \pm 0.14$  to  $0.39 \pm$  318  
 $0.15$ ) observed at the plateau since observations started at Santa 319  
 Ana (Fig. 7). In 2018, the gas composition remained  $H_2O$ -rich 320  
 ( $H_2O/SO_2$  between  $32 \pm 18$  and  $177 \pm 11$ ), and the  $H_2S/SO_2$  ratio 321  
 varied between  $0.08 \pm 0.07$  and  $0.1 \pm 0.07$  (Table 1).  $H_2S$  was 322  
 below detection limit in May and June 2018. 323

**Discussion**

The Santa Ana crater lake has frequently witnessed phreatic 325  
 and phreatomagmatic eruptions in historical time, most recently in 2005 and 2007, and thus poses a potential 326  
 threat to local inhabitants and numerous visitors. Colvin et al. (2013) suggested that the crater lake entered 327  
 a new period of quiescence in early 2008, though with a higher steady-state mass/energy input than before the 328  
 2005–2007 eruptions. This quiescent phase was confirmed by the low levels of background seismicity and 329  
 $SO_2$  fluxes (Fig. 4) and by the relatively stable lake temperature and chemistry (Fig. 2) (Colvin et al. 2013). The 330  
 most recent data suggest, however, that a new cycle of lake surface temperature increase, and pH decrease, 331  
 started sometime between late 2010 and early 2017 (Fig. 2). Although trends in lake water chemistry are difficult 332  
 to interpret, due to the discontinuous nature of the dataset, sulfate and chloride concentrations were found to be 333  
 334  
 335  
 336  
 337  
 338  
 339  
 340  
 341

**Fig. 9** Variations in **a** the lake level, **b** CO<sub>2</sub>/SO<sub>2</sub> ratios, and **c** CO<sub>2</sub> fluxes, between March 2017 and June 2018 (data from Table S1 and Table 1). Dashed lines in **b** are the CO<sub>2</sub>/SO<sub>2</sub> gas ratios of high-temperature fumaroles in 2002 (sampled by T.F.)



342 higher in 2014 than in 2010 and peaked in 2017 (Fig. 2).  
 343 Overall, this evolution in lake water chemistry and temper-  
 344 ature may potentially imply renewed unrest and there-  
 345 fore needs careful scrutiny.

346 Our lake gas plume results thus contribute to our under-  
 347 standing of the Santa Ana crater lake. Although the lack of  
 348 similar data prior to 2017 (and especially prior to the 2005–  
 349 2007 eruptions) partially hampers our interpretation, our gas  
 350 data nevertheless contribute to assessing and hypothesizing on  
 351 the current activity level at the crater lake. An important ob-  
 352 servation in this study is that the compositional features of the  
 353 Santa Ana plume are heterogeneous, in both space and time.

354 **Spatial variability**

355 Measurements taken in 2017 from three distinct locations  
 356 (rim, plateau, and shore), at different distances from the gas  
 357 emission source (i.e., mainly the crater lake), imply some spa-  
 358 tial heterogeneity in plume composition. At the rim, gas ob-  
 359 servations are complicated by the highly diluted nature of the

plume detected; we consider the derived ratios strongly affected  
 by analytical uncertainty, e.g., due to the difficulty in res-  
 olving volcanic gases over atmospheric background, especially  
 for H<sub>2</sub>O, CO<sub>2</sub>, and H<sub>2</sub> (Fig. 5a). We hence conclude that the  
 rim is not an ideal monitoring site, at least with the current  
 state of activity at Santa Ana. The plateau, instead, is a far  
 more promising monitoring site because, in addition to being  
 safer and more accessible than the crater lake shore (Fig. 3),  
 it is also systematically fumigated by a relatively dense plume  
 (SO<sub>2</sub> at levels of tens of ppm). Importantly, our filtered  
 dataset, in which measurements taken at higher plume density  
 (SO<sub>2</sub> > 7 ppm) are considered (Table 1; Fig. 9), confirms that  
 CO<sub>2</sub>/SO<sub>2</sub> ratios exhibit overlapping ranges at plateau and  
 shore in all campaigns (March and June 2017 and November  
 2018). The similarity of CO<sub>2</sub>/SO<sub>2</sub> ratios (Fig. 10) at the  
 plateau and shore confirms the utility of the latter site for  
 monitoring. In contrast, H<sub>2</sub>/SO<sub>2</sub> ratios at the plateau and at  
 the shore do not match in both the March and June 2017  
 datasets, even in the filtered dataset (Table 1), and are sys-  
 tematically higher at the former, more distal site. We are con-  
 fident that this

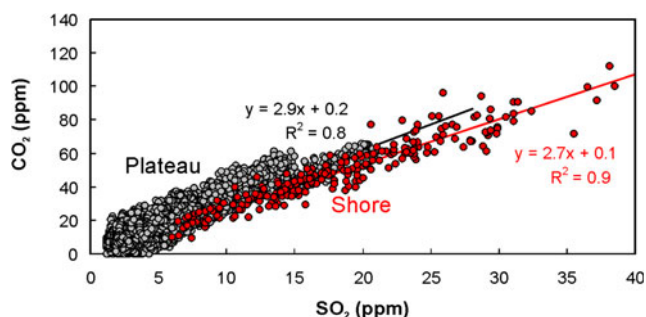


**Fig. 10** CO<sub>2</sub> vs. SO<sub>2</sub> correlation plot for the simultaneous plateau (gray) and shore (red) Multi-GAS observations taken on November 28, 2018. The two derived CO<sub>2</sub>/SO<sub>2</sub> ratios overlap within uncertainty

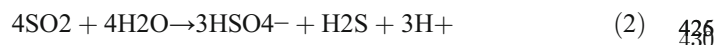
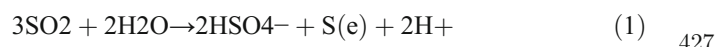
380 spatial change in composition (H<sub>2</sub>/SO<sub>2</sub> ratio) cannot reflect  
 381 analytical uncertainties, at least in the filtered dataset that in-  
 382 cludes only measurements taken in dense plume conditions, where ratios are independent of SO<sub>2</sub> concentrations (see Fig.  
 383 8). Also, SO<sub>2</sub> and H<sub>2</sub> are thought (Aiuppa et al. 2005b, 2011;  
 384 Ehhalt and Rohrer 2009) to behave conservatively (i.e., to be  
 385 poorly reactive) over the short travel times of seconds to tens  
 386 of seconds associated with plume transport from the lake  
 387 shore to the plateau. As such, we consider it unlikely that the  
 388 H<sub>2</sub>/SO<sub>2</sub> ratio difference between the shore and plateau is due  
 389 to in-plume chemical processing. We find it, instead, more  
 390 likely that the compositional change between plateau and  
 391 shore reflect some additional H<sub>2</sub> contributions from other  
 392 sources, perhaps weakly degassing hydrothermal fumaroles  
 393 and steaming ground on the inner crater slope (Figs. 7 and  
 394 8). We suggest that these additional, diffuse gases (see Fig.  
 395 8) become mixed with the lake plume during plume transport  
 396 between emission from the lake surface and measurement at  
 397 the plateau, thus justifying the H<sub>2</sub> excess seen at the plateau  
 398 (Figs. 7 and 8 and Table 1). This *diffuse degassing* source (see  
 399 Fig. 8) may also explain the H<sub>2</sub>-CO<sub>2</sub>-enriched (relative to *lake*  
 400 *degassing*; Fig. 8) compositions of dilute (SO<sub>2</sub> < 7 ppm) pla-  
 401 teau and rim plumes.  
 402

### 403 Temporal trends

404 In addition to spatial heterogeneity, our measurements also  
 405 highlight important temporal changes in gas composition  
 406 (Fig. 9). We observed that the CO<sub>2</sub>/SO<sub>2</sub> ratio decreased by  
 407 more than one order of magnitude in 1 year, from  
 408 March 2017 (shore 31.0 ± 13.7; plateau 37.2 ± 9.7) to June–  
 409 November 2018 (< 3.0 at both shore and plateau) (Fig. 9). The  
 410 H<sub>2</sub>/SO<sub>2</sub> ratios at the plateau were also lower (and far less  
 411 variable) in May–June 2018 than in March 2017, both in the  
 412 total (Figs. 7 and 8) and filtered (Table 1) datasets. Overall,  
 413 these observations imply a gas composition becoming more  
 414 SO<sub>2</sub>-rich over time. H<sub>2</sub>S has remained a minor sulfur com-  
 415 pound throughout the entire period of observation (Table 1).

416 In lake gas plumes, the S composition and flux reflect a  
 417 complex and temporally variable balance between sulfur input

flux into the lake via the magmatic/hydrothermal gas supply at 418  
 the lake-bottom, gas scavenging by lake water as dissolved 419  
 sulfur and/or mineral precipitates, and surface gas release (as 420  
 either SO<sub>2</sub> or H<sub>2</sub>S). Gas-water-rock reactions in the lake re- 421  
 move sulfur from the input gas via (Kusakabe et al. 2000; 422  
 Christenson and Tassi 2015; Delmelle and Bernard 2015; de 423  
 Moor et al. 2016a); 424



433 in which S(e) is elemental sulfur. The increasingly 434  
 SO<sub>2</sub>-rich compositions of the Santa Ana lake plume gas 435  
 in 2018, relative to 2017, suggest a shift of the above 436  
 reactions toward the left, i.e., they indicate a lower con- 437  
 sumption of the reagents during gas-water-rock reactions 438  
 into the lake. A reduced SO<sub>2</sub> dissolution into the lake 439  
 explains the tendency of our lake plume gas to become 440  
 increasingly SO<sub>2</sub>-rich (i.e., more magmatic in nature). The 441  
 low H<sub>2</sub>S contents in the Santa Ana lake plume imply that 442  
 reaction mechanisms (1) and/or (2) are most likely in- 443  
 volved because the reversal of reaction (3) should lead 444  
 to H<sub>2</sub>S formation, which is not observed. 445

The composition of the Santa Ana input gas in 2017–2018 446  
 is unknown, in view of the lack of measurable fumaroles. 447  
 However, two high-temperature (400 to 875 °C) gas samples 448  
 were collected at Santa Ana by one of us (T.F.) in June 2002. 449  
 Assuming these compositions as representative of the current 450  
 (2017–2018) magmatic gas input into the lake (Figs. 7 and 9) 451  
 confirms that lake plume gas has become increasingly more 452  
 magmatic in nature in 2018, relative to 2017. The triangular 453  
 plots of Fig. 11 additionally support a progressive evolution of 454  
 the Santa Ana plume gas toward more magmatic composi- 455  
 tions. These plots compare the Santa Ana lake gas composi- 456  
 tion of this study with (i) the magmatic fumaroles in 2002 and 457  
 (ii) the compositions of lake gas plumes recently obtained at 458  
 other quiescent and/or recently active crater lakes worldwide 459  
 (see caption for data sources). The plots confirm that, over the 460  
 year of observations (2017–2018), the Santa Ana lake gas 461  
 evolved in composition from CO<sub>2</sub>-H<sub>2</sub>-rich and S-poor to more 462  
 S-rich, encompassing an intermediate position between the 463  
 CO<sub>2</sub>-H<sub>2</sub>-H<sub>2</sub>S-rich lake plumes as seen at “quiescent” crater 464  
 lakes (e.g., El Chichón and Viti; Hasselle et al. 2018), and 465  
 the far more SO<sub>2</sub>-rich plumes issuing from “recently erupting” 466  
 crater lakes (Yudamari, Copahue, Poás, and Rincón de la 467  
 Vieja; Shinohara et al. 2015; Tamburello et al. 2015; de 468  
 Moor et al. 2016a, 2019; Battaglia et al. 2019) (Fig. 11). The 469  
 2018 lake plume is also approaching the “magmatic” compo- 470  
 sition of the high-T (875 °C) fumarole sampled in the restless 471  
 Santa Ana crater in 2002. 472



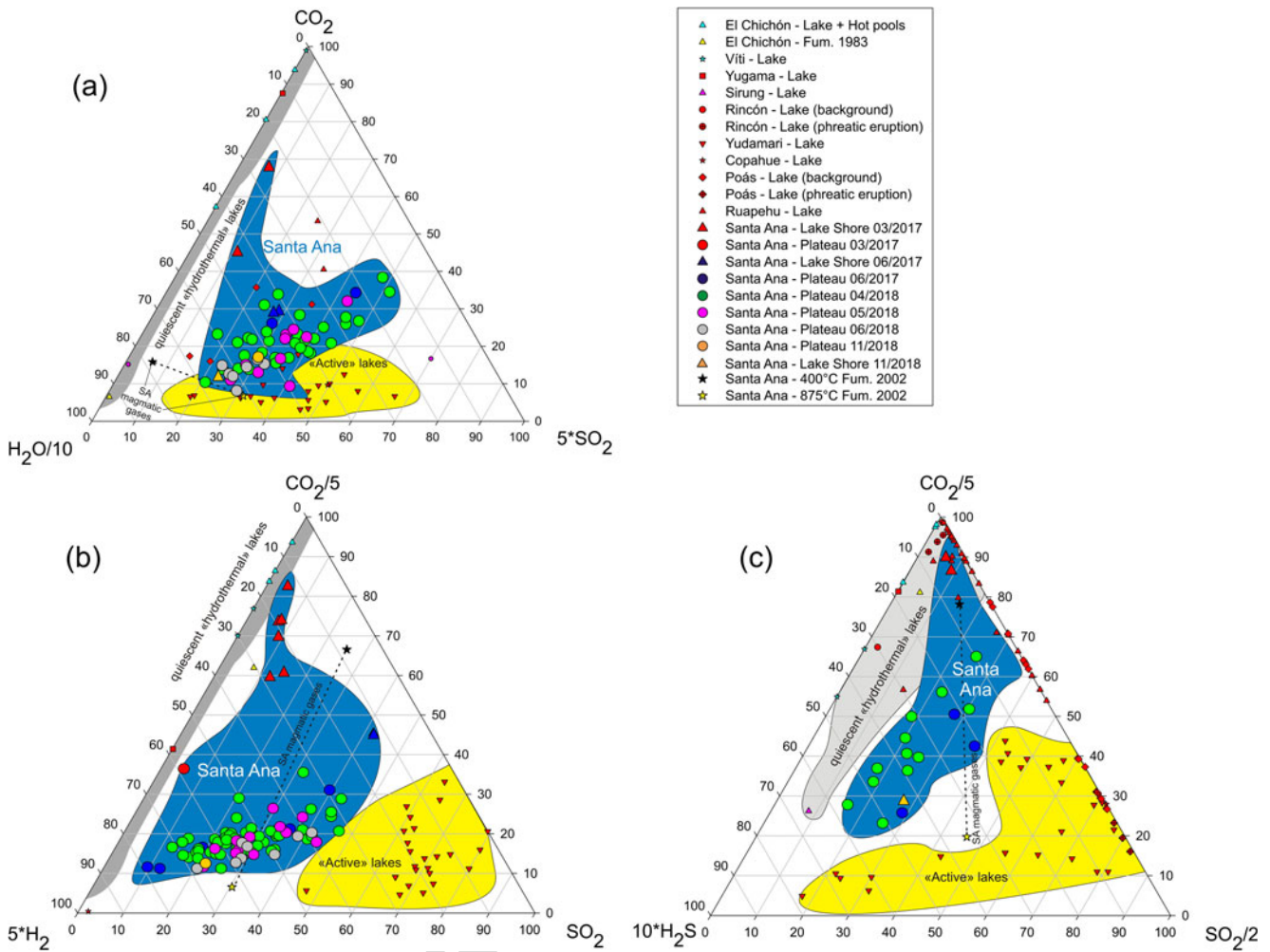


**Fig. 11** Triangular plots ( $\text{H}_2\text{O}-\text{CO}_2-\text{SO}_2$  (a),  $\text{CO}_2-\text{H}_2-\text{SO}_2$  (b), and  $\text{CO}_2-\text{H}_2\text{S}-\text{SO}_2$ (c)) illustrating the temporal evolution of the chemical composition of the Santa Ana crater lake gas plume. The Santa Ana plume data (filtered dataset only; data from Table S1 filtered at the  $\text{SO}_2$  threshold of  $\geq 7$  ppmv) are compared with a selection of crater lake plume compositions from El Chichón (Mexico; Hasselle et al. 2018), Viti (Iceland; Hasselle et al. 2018), Yugama (Kusatsu-Shirane volcano, Japan; Hasselle 2019), Yudamari (Aso volcano, Japan; Shinohara et al. 2015), Copahue (Argentina-Chile; Tamburello et al. 2015), Ruapehu

(New Zealand; Hasselle 2019), Sirung (Bani et al. 2017), Poás (de Moor et al. 2016a), and Rincón de la Vieja (Battaglia et al. 2018). The 2018 Santa Ana plume gases have increasingly become more magmatic (more similar to the 2002 high-T fumaroles data of T.F.) with respect to the 2017 plume gases. Santa Ana crater lake gas occupies an intermediate position (blue-colored field) between “quiescent hydrothermal lakes” (El Chichón, Viti and Yugama; gray field) and “active lakes” (Copahue, Yudamari, Kawah Ijen; yellow field)

**473 Internal vs. external controls on lake gas evolution**

474 The next obvious question is: what is the possible driver for the  
 475 observed variations in gas compositions, and to what extent  
 476 these signals represent potential hints for renewed volcanic un-  
 477 rest?  $\text{SO}_2$  dissolution into volcanic crater lakes involves non-  
 478 equilibrium, kinetically controlled gas-water-solid reactions  
 479 (Kusakabe et al. 2000; Miyabuchi and Terada 2009;  
 480 Christenson and Tassi 2015; de Moor et al. 2016a). Hence, since  
 481 timing of gas-water interaction is the key factor, reduced sulfur  
 482 absorption and scrubbing in 2018, as suggested by declining  
 483  $\text{CO}_2/\text{SO}_2$  ratios, implies faster gas transit through the lake.

484 The gas transit time in a volcanic lake and, hence, the  
 485 possible timescales of gas-water interactions scale to lake

486 volume and depth (e.g., the deeper the lake, the longer the  
 487 gas residence time) (Christenson and Tassi 2015) and input  
 488 gas flux (de Moor et al. 2016a). Visual observations at the  
 489 crater rim (Fig. 9) indicate that the Santa Ana crater lake level  
 490 fell in 2018, relative to 2017. Our records (Fig. 2b) highlight  
 491 that the crater lake level dropped by a maximum  $\sim 3$  m  
 492 between March and June 2017 and remained similarly low, or  
 493 lower (Fig. 9), in April–May 2018. The dropping lake level in  
 494 late 2017 to early 2018 is possibly part of a longer-term dry-  
 495 ing-out trend that started sometime in 2011 (Fig. 2b). Image-  
 496 based, semi-quantitative estimates of relative lake level chang-  
 497 es (Fig. 2b), based on relative level variations with respect to a  
 498 reference level, show in fact that while the lake essentially  
 499 rose in level from 2007 to 2010, the trend reversed since

2011, when relative level changes have been either null (e.g., 2011–2013) or negative (e.g., 2015). The negative lake level fluctuations observed since June 2017 are, in particular, unique in the recent (post-2000) Santa Ana record and also correspond to a phase of peaking lake temperature, salinity, and acidity (Fig. 2c, d). As a result, we propose that the post-June 2017 reduced lake volume caused a general decrease in the gas residence time in the lake, leading to less efficient sulfur reactions with lake water and ultimately to more SO<sub>2</sub>-rich lake gas plume compositions.

Precipitation records in the Santa Ana area (Fig. 2a) suggest that the recent decrease in crater lake volume may have been caused, at least partially, by a decreased meteoric water supply to the lake itself. Precipitation in the Santa Ana area nearly halved in 2018 relative to 2010–2011 and was ~ 15% lower than in 2017 (Fig. 2a). It is therefore likely that the reduced meteoric water influx contributed to reducing the crater lake volume. This conclusion is consistent with recent modelling work (Terada and Hashimoto 2017) demonstrating that low levels of precipitation can cause sizeable changes in crater lake temperature and composition, even at constant sub-aqueous gas input into the lake.

However, our gas flux measurements (Table 1) suggest that, in addition to reduced meteoric precipitations, an “internal” volcano-driven trigger was also likely at play. During our Multi-GAS surveys, the SO<sub>2</sub> fluxes were the highest in March 2017 (with daily averages of 240 and 329 t/day on March 7 and 8, respectively; see Table 1). By scaling our measured daily averaged lake plume gas ratios to the daily mean SO<sub>2</sub> fluxes, we can also calculate the H<sub>2</sub>O, CO<sub>2</sub>, H<sub>2</sub>, and H<sub>2</sub>S fluxes (Table 1). Results demonstrate that fluxes of H<sub>2</sub>O (13,825–17,565 t/day), CO<sub>2</sub> (5117 to 12,320 t/day), and total volatiles (TV 20,217–30,225 t/day; the total volatile flux is the sum of H<sub>2</sub>O + CO<sub>2</sub> + SO<sub>2</sub> + H<sub>2</sub> fluxes in our specific case) were one order of magnitude higher in March 2017 than at any time since (H<sub>2</sub>O 892–9483; CO<sub>2</sub> 118–485; TV 615–10167 t/day; Table 1). These results thus suggest that an increased gas supply from the sub-limnic magmatic-hydrothermal system (as implied by the anomalously high March 2017 fluxes) was a likely additional causal factor in driving the lake toward dryness. We propose that the elevated gas supply and, hence, heat transfer into the lake caused more intense lake evaporation (resulting in decreasing lake volume; Fig. 2b) and heating (where the lake warmed-up in late 2017; Fig 2c). We also argue that, because of the relatively high lake level in March 2017, the majority of the magmatic/hydrothermal S and Cl input was initially dissolved into the lake, thus justifying the anomalously elevated dissolved SO<sub>4</sub> and Cl (Fig. 2d) and the SO<sub>2</sub>-poor lake plume gas (Fig. 9). In the following months, however, the lake level drop caused more rapid fluxing of gas through the lake, reducing the time-scales of gas-water interactions and, thus, the lake’s ability to scrub magmatic sulfur, ultimately determining a more

magmatic (SO<sub>2</sub>-rich) lake gas plume in late 2017 and in 2018. The lack of any sizeable change in seismicity (Fig. 4) perhaps suggests that the escalation in deep gas supply was not elevated enough to cause pressurization/fracturing of the sub-limnic hydrothermal-magmatic system.

**Conclusions and implications for monitoring**

Our novel gas plume results highlight the dynamic nature of the Santa Ana crater lake and reveal rapid compositional evolution in only 2 years of observation (2017–2018). However, available information on gas plume chemistry is too restricted in time to allow firm conclusions to be made on the current state of activity of the volcano. In particular, we cannot determine when the phase of elevated total volatile fluxes we observed in March 2017 actually started. Notwithstanding this, our results clearly show that the lake plume gas became increasingly more SO<sub>2</sub>-rich, and therefore more magmatic in nature, in late 2017 and 2018. These gas variations have been paralleled by consistent variations in lake water chemistry and physical parameters, including increased lake temperature, acidity, and salinity, and a reduction in lake level and volume.

We propose these variations have been caused by a combination of external and internal processes, such as a decrease in precipitation and increased mass/heat supply at the lake bottom in March 2017, or before. In our interpretation, a ~ 15% drop in precipitation, and the elevated magmatic/hydrothermal fluid supply in March 2017, combined to reduce the lake volume. In turn, this resulted in a shortened magmatic gas transit time through the lake water. This lead to a reduction of magmatic sulfur reacting with lake water and ultimately to a more SO<sub>2</sub>-rich gas plume.

The dynamic evolution of degassing at Santa Ana volcano, highlighted in the present study, argues for the need of further observations and careful scrutiny of water/gas compositional features in the very near future. Comparison with gas plume data from other crater lakes worldwide demonstrates that the 2018 Santa Ana lake gas is intermediate in composition between the CO<sub>2</sub>-H<sub>2</sub>-H<sub>2</sub>S-rich lake plumes seen at “quiescent” crater lakes (e.g., El Chichón in Mexico), and the by-far more SO<sub>2</sub>-rich plumes issuing from “recently erupting” lakes (e.g., Poás in Costa Rica). As such, any additional compositional change toward the SO<sub>2</sub>-rich magmatic gas end-member should seriously be considered as evidence of activity escalation. At Laguna Caliente (Poás, Costa Rica), increasing SO<sub>2</sub> typically peaks prior to phreatic/phreato-magmatic eruptions (de Moor et al. 2016a, 2019; Stix and de Moor 2018), reflecting increasing magmatic gas influx into the lake. Although this critical situation seems not to have yet been reached at Santa Ana, our results underpin the need of reinforced volcano monitoring at this potentially hazardous volcano.

- 602 **Acknowledgments** This research was funded by the Agenzia italiana per  
603 la cooperazione allo sviluppo (AICS) via the project RIESCA. A.A. ac-  
604 knowledges funding from the Deep Carbon Observatory and from Miur  
605 (Grant n. 2017LMNLAW). The manuscript benefited from comments  
606 from A. Terada and one anonymous reviewer. Associate Editor P.  
607 Allard and Editor-in-Chief A. Harris fine-tuned the final manuscript.
- 608
- 609 **References**
- 610 Augusto M, Varekamp J (2016) The Copahue volcanic-hydrothermal sys-  
611 tem and applications for volcanic surveillance. In: In Copahue  
612 Volcano. Springer, Berlin, pp 199–238
- 613 Aiuppa A, Federico C, Giudice G, Gurrieri S (2005a) Chemical mapping  
614 of a fumarolic field: la Fossa crater, Vulcano Island (Aeolian Islands,  
615 Italy). *Geophys Res Lett* 32(13)
- 616 Aiuppa A, Inguaggiato S, McGonigle AJS, O'Dwyer M, Oppenheimer C,  
617 Padgett MJ, Rouwet D, Valenza M (2005b) H<sub>2</sub>S fluxes from Mt.  
618 Etna, Stromboli, and Vulcano (Italy) and implications for the sulfur  
619 budget at volcanoes. *Geochim Cosmochim Acta* 69:1861–1871.  
620 <https://doi.org/10.1016/j.gca.2004.09.018>
- 621 Aiuppa A, Federico C, Giudice G, Giuffrida G, Guida R, Gurrieri S,  
622 Liuzzo M, Moretti R, Papale P (2009) The 2007 eruption of  
623 Stromboli volcano: insights from real-time measurement of the vol-  
624 canic gas plume CO<sub>2</sub>/SO<sub>2</sub> ratio. *J Volcanol Geotherm Res* 182:221–  
625 230
- 626 Aiuppa A, Shinohara H, Tamburello G, Giudice G, Liuzzo M, Moretti R  
627 (2011) Hydrogen in the gas plume of an open-vent volcano, Mount  
628 Etna, Italy. *J Geophys Res Solid Earth* 116(B10)
- 629 Aiuppa A, de Moor JM, Arellano S, Coppola D, Francofonte V, Galle B,  
630 Giudice G, Liuzzo M, Mendoza E, Saballos A, Tamburello G,  
631 Battaglia A, Bitetto M, Gurrieri S, Laiolo M, Mastroli A, Moretti  
632 R (2018) Tracking formation of a lava lake from ground and space:  
633 Masaya volcano (Nicaragua), 2014–2017. *Geochem Geophys*  
634 *Geosyst* 19. <https://doi.org/10.1002/2017GC007227>
- 635 Bani P, Alfianti H, Aiuppa A, Oppenheimer C, Sitingjak P, Tsanev V, Saing  
636 UB (2017) First study of the heat and gas budget for Sirung volcano.  
637 *Indonesia Bull Volcanol* 79(8):60
- 638 Battaglia A, Bitetto M, Aiuppa A, Rizzo AL, Chigna G, Watson IM,  
639 D'Aleo R, Juárez Cacao FJ, de Moor MJ (2019) Insights into the  
640 mechanisms of phreatic eruptions from continuous high frequency  
641 volcanic gas monitoring: Rincón de la Vieja Volcano, Costa Rica.  
642 *Front Earth Sci* 6:247. <https://doi.org/10.3389/feart.2018.00247>
- 643 Bernard A, Escobar CD, Mazot A, Gutiérrez RE (2004) The acid volcanic  
644 lake of Santa Ana volcano, El Salvador. *Special Pap-Geol Soc Am*  
645 375:121–134
- 646 Cabassi J, Capeccchiacci F, Magi F, Vaselli O, Tassi F, Montalvo F,  
647 Esquivel I, Grassa F, Caprai A (2019) Water and dissolved gas  
648 geochemistry at Coatepeque, Ilopango and Channico volcanic lakes  
649 (El Salvador, Central America). *J Volcanol Geotherm Res* 378:1–15.  
650 <https://doi.org/10.1016/j.jvolgeores.2019.04.009>
- 651 Capaccioni B, Rouwet D, Tassi F (2017) HCl degassing from extremely  
652 acidic crater lakes: preliminary results from experimental determi-  
653 nations and implications for geochemical monitoring. In: Ohba, T.,  
654 Capaccioni, B. & Caudron, C. (eds) *Geochemistry and geophysics*  
655 *of Active Volcanic Lakes*. Geological Society, London, Special  
656 *Publications* 437: 97–106.
- 657 Carr MJ (1984) Symmetrical and segmented variation of physical and  
658 geochemical characteristics of the Central American volcanic front.  
659 *J Volcanol Geotherm Res* 20(3-4):231–252
- 660 Carr MJ, Pontier NK (1981) Evolution of a young parasitic cone towards  
661 a mature central vent; Izalco and Santa Ana volcanoes in El  
662 Salvador, Central America. *J Volcanol Geotherm Res* 11(2-4):277–  
663 292
- 664 Caudron C, Lecocq T, Syahbana DK, McCausland W, Watlet A,  
665 Camelbeeck T, Bernard A, Surono (2015) Stress and mass changes  
666 at a “wet” volcano: example during the 2011–2012 volcanic unrest at  
667 Kawah Ijen volcano (Indonesia). *J Geophys Res* 120(5):5117–5134.  
668 <https://doi.org/10.1002/2014JB011590>
- 669 Caudron C, Mauri G, Williams-Jones G, Lecocq T, Syahbana DK, De  
670 Plaen R, Peiffer L, Bernard A, Saracco G (2017) New insights into  
671 the Kawah Ijen hydrothermal system from geophysical data. In:  
672 Ohba, T., Capaccioni, B. & Caudron, C. (eds) *Geochemistry and*  
673 *geophysics of Active Volcanic Lakes*. Geological Society, London,  
674 *Special Publications* 437: 57–72.
- 675 Colvin AS (2008) Crater lake evolution during volcanic unrest: case  
676 study of the 2005 phreatic eruption at Santa Ana volcano, El  
677 Salvador, 195 pp (MS thesis, Mich. Technol. Univ., Houghton).
- 678 Colvin AS, Rose WI, Varekamp JC, Palma JL, Escobar D, Gutiérrez E,  
679 Montalvo F, Maclean A (2013) Crater lake evolution at Santa Ana  
680 Volcano (El Salvador) following the 2005 eruption. *Understanding*  
681 *Open-Vent Volcanism and Related Hazards*. Geological Society of  
682 *America. Special Pap* 498:23–44
- 683 Christenson BW (2000) Geochemistry of fluids associated with the  
684 1995–1996 eruption of Mt. Ruapehu, New Zealand: signatures  
685 and processes in the magmatic-hydrothermal system. *J Volcanol*  
686 *Geotherm Res* 97:1–30
- 687 Christenson B, Tassi F (2015) Gases in volcanic lake environments. In: In  
688 *Volcanic lakes*. Springer, Berlin, pp 125–153
- 689 Christenson B, Németh K, Rouwet D, Tassi F, Vandemeulebrouck J,  
690 Varekamp JC (2015) Volcanic lakes. In: In *Volcanic lakes*.  
691 Springer, Berlin, pp 1–20
- 692 Christenson B, Reyes AG, Young R, Moebis A, Sherburn S, Cole-Baker  
693 J, Britten K (2010) Cyclic processes and factors leading to phreatic  
694 eruption events: insights from the 25 September 2007 eruption  
695 through Ruapehu Crater Lake, New Zealand. *J Volcanol Geotherm*  
696 *Res* 191(1-2):15–32
- 697 Delmelle P, Bernard A (2015) The remarkable chemistry of sulfur in  
698 hyper-acid crater lakes: a scientific tribute to Bokuichiro Takano  
699 and Minoru Kusakabe. In: In *Volcanic Lakes*. Springer, Berlin, pp  
700 239–259
- 701 DeMets C, Gordon RG, Argus DF, Stein S (1990) Current plate motions.  
702 *Geophys J Int* 101(2):425–478
- 703 de Moor JM, Aiuppa A, Pacheco J, Avarad G, Kern C, Liuzzo M, Martínez  
704 M, Giudice G, Fischer TP (2016a) Short-period volcanic gas pre-  
705 cursors to phreatic eruptions: insights from Poás Volcano, Costa  
706 Rica. *Earth Planet Sci Lett* 442:218–227
- 707 de Moor JM, Aiuppa A, Avarad G, Wehrmann H, Dunbar N, Muller C,  
708 Tamburello G, Giudice G, Liuzzo M, Moretti R, Conde V, Galle B  
709 (2016b) Turmoil at Turrialba Volcano (Costa Rica): degassing and  
710 eruptive processes inferred from high-frequency gas monitoring. *J*  
711 *Geophys Res Solid Earth* 121(8):5761–5775
- 712 de Moor JM, Stix J, Avarad G, Muller C, Corrales E, Diaz JA, Alan A,  
713 Brenes J, Pacheco J, Aiuppa A, Fischer TP (2019) Insights on  
714 hydrothermal-magmatic interactions and eruptive processes at  
715 Poás Volcano (Costa Rica) from high-frequency gas monitoring  
716 and drone measurements. *Geophys Res Lett* 46(3):1293–1302.  
717 <https://doi.org/10.1029/2018GL080301>
- 718 Ehhalt DH, Rohrer F (2009) The tropospheric cycle of H<sub>2</sub>: a critical  
719 review. *Tellus Ser B Chem Phys Meteorol* 61(3):500–535
- 720 Fischer TP, Chiodini G (2015) Volcanic, magmatic and hydrothermal gas  
721 discharges. *Encyclopaedia of Volcanoes*, 2nd ed., pp. 779–797  
722 <https://doi.org/10.1016/B978-0-12-385938-9.00045-6>.
- 723 Galle B, Johansson M, Rivera C, Zhang Y, Kihlman M, Kern C,  
724 Lehmann T, Platt U, Arellano S, Hidalgo S (2010) Network for  
725 Observation of Volcanic and Atmospheric Change (NOVAC)-A  
726 global network for volcanic gas monitoring: network layout and  
727 instrument description. *J Geophys Res* 115.

- 728 Gunawan H, Caudron C, Pallister J, Primulyana S, Christenson B, 770  
 729 Mccausland W, Van Hinsberg V, Lewicki J, Rouwet D, Kelly P, 771  
 730 Kern C, Werner C, Johnson JB, Utami SB, Syahbana DK, Saing 772  
 731 U, Suparjan PBH, Sealing C, Martinez Cruz M, Maryanto S, Bani P, 773  
 732 Laurin A, Schmid A, Bradley K, Nandaka IGMA, Hendrasto M 774  
 733 (2016) New insights into Kawah Ijen's volcanic system from the 775  
 734 wet volcano workshop experiment. *Geol Soc Lond, Spec Publ* 776  
 735 437:35–56
- 736 Gutiérrez RE, Escobar CD (1994) Crisis en la actividad del volcán de 777  
 737 Santa ana (Ilamatepec), del 22 de Julio al 21 de Agosto 1992. Centro 778  
 738 de Investigaciones Geotecnicas, unpublished report, El Salvador, p 779  
 739 14
- 740 GVP (Global Volcanism Program), (2018) Smithsonian Institution. 780  
 Q11 741 <https://volcano.si.edu/> 781
- 742 Halsor SP, Rose WI (1988) Common characteristics of paired volcanoes 782  
 743 in northern Central America. *J Geophys Res Solid Earth* 93(B5): 783  
 744 4467–4476
- 745 Hasselle N (2019) Gas in volcanic lakes: from dissolved gases to lake gas 784  
 746 plumes. PhD dissertation, University of Palermo.
- 747 Hasselle N, Rouwet D, Aiuppa A, Jácome-Paz MP, Pfeiffer M, Taran Y, 785  
 748 Champion R, Bitetto M, Giudice G, Bergsson B (2018) Sulfur 786  
 749 degassing from steam-heated crater lakes. *El Chichón (Chiapas,* 787  
 750 *Mexico) and Víti (Iceland) Geophysical Research Letters* 45(15): 788  
 751 7504–7513. <https://doi.org/10.1029/2018GL079012> 789
- 752 Kusakabe M, Komoda Y, Takano B, Abiko T (2000) Sulfur isotopic 790  
 753 effects in the disproportionation reaction of sulfur dioxide in hydro- 791  
 754 thermal fluids: implications for the  $\delta^{34}\text{S}$  variations of dissolved bi- 792  
 755 sulfates and elemental sulfur from active crater lakes. *J Volcanol* 793  
 756 *Geotherm Res* 97(1–4):287–307
- 757 Laiolo M, Coppola D, Barahona F, Benitez J, Cigolini C, Escobar D, 794  
 758 Funes R, Gutiérrez E, Henriquez B, Hernández A, Montalvo F, 795  
 759 Olmos R, Ripepe M, Finizola A (2017) Evidences of volcanic unrest 796  
 760 on high-temperature fumaroles by satellite thermal monitoring: the 797  
 761 case of Santa Ana volcano, El Salvador. *J Volcanol Geotherm Res* 798  
 762 340:170–179
- 763 Miyabuchi Y, Terada A (2009) Subaqueous geothermal activity revealed 799  
 764 by lacustrine sediments of the acidic Nakadake crater lake, Aso 800  
 765 Volcano, Japan. *J Volcanol Geotherm Res* 187:140–145. <https://doi.org/10.1016/j.jvolgeores.2009.08.001> 801
- 766 Mooser F, Meyer-Abich H, McBirney AR (1958) Catalogue of the active 802  
 767 volcanoes and Solfatara fields of Central America. *Int Volcanol* 803  
 768 *Assoc.* 804  
 769 813
- Ohba T, Hirabayashi JI, Nogami K (2008) Temporal changes in the 770  
 chemistry of lake water within Yugama Crater, Kusatsu-Shirane 771  
 Volcano, Japan: implications for the evolution of the magmatic hy- 772  
 drothermal system. *J Volcanol Geotherm Res* 178(2):131–144 773
- Olmos R et al (2007) Anomalous emissions of  $\text{SO}_2$  during the recent 774  
 eruption of Santa Ana volcano, El Salvador, Central America. 775  
*Pure Appl Geophys* 164(12):2489–2506 776
- Pullinger CR (1998) Evolution of the Santa Ana volcanic complex, El 777  
 Salvador, 145 pp (MS thesis, Mich. Technol. Univ., Houghton). 778
- Rouwet D, Mora-Amador R, Ramírez-Umaña CJ, González G, 779  
 Inguaggiato S (2016) Dynamic fluid recycling at Laguna Caliente 780  
 (Poás, Costa Rica) before and during the 2006-ongoing phreatic 781  
 eruption cycle (2005–10). *Geol. Soc. London, Special Publications* 782  
 437 (Eds. Ohba, T., Capaccioni, B., Caudron, C.) doi: [https://doi.](https://doi.org/10.1144/SP437.11) 783  
[org/10.1144/SP437.11](https://doi.org/10.1144/SP437.11) 784
- Rowe GL, Ohsawa S, Takano B, Brantley SL, Fernández JF, Barquero J 785  
 (1992) Using crater lake chemistry to predict volcanic activity at 786  
 Poás volcano, Costa Rica. *Bull Volcanol* 54(6):494–503 787
- Scolamacchia T, Pullinger C, Caballero L, Montalvo F, Orosco LEB, 788  
 Hernández GG (2010) The 2005 eruption of Ilamatepec (Santa 789  
 Ana) volcano, El Salvador. *J Volcanol Geotherm Res* 189(3):291– 790  
 318 791
- Shinohara H (2005) A new technique to estimate volcanic gas composi- 792  
 tion: plume measurements with a portable multi-sensor system. *J* 793  
*Volcanol Geotherm Res* 143(4):319–333 794
- Shinohara H, Yoshikawa S, Miyabuchi Y (2015) Degassing activity of a 795  
 volcanic crater lake: volcanic plume measurements at the Yudamari 796  
 crater lake, Aso volcano, Japan. In: *In Volcanic lakes*. Springer, 797  
 Berlin, pp 201–217 798
- Stix J, de Moor JM (2018) Understanding and forecasting phreatic eruptions 799  
 driven by magmatic degassing. *Earth, Planets and Space* 70(1) 800
- Takano B, Ohsawa S, Glover RB (1994) Surveillance of Ruapehu crater 801  
 lake, New Zealand, by aqueous polythionates. *J Volcanol Geotherm* 802  
*Res* 60(1):29–57 803
- Terada A, Hashimoto T (2017) Variety and sustainability of volcanic 804  
 lakes: response to subaqueous thermal activity predicted by a numerical 805  
 model. *J. Geophys. Res. Solid Earth* 122:6108–6130. 806  
<https://doi.org/10.1002/2017JB014387> 807
- Tamburello G, Agosto M, Caselli A, Tassi F, Vaselli O, Calabrese S, 808  
 Rouwet D, Capaccioni B, Di Napoli R, Cardellini C, Chiodini G, 809  
 Bitetto M, Brusca L, Bellomo S, Aiuppa A (2015) Intense magmatic 810  
 degassing through the lake of Copahue volcano, 2013–2014. *J* 811  
*Geophys Res Solid Earth* 120(9):6071–6084 812

## AUTHOR QUERIES

### AUTHOR PLEASE ANSWER ALL QUERIES.

- Q1. Please check if the affiliations are captured and presented correctly.
- Q2. Please check if the section headings are assigned to appropriate levels.
- Q3. The citation “Fischer and Chiodini 2017” has been changed to “Fischer and Chiodini, 2015” to match the author name/date in the reference list. Please check if the change is fine in this occurrence and modify the subsequent occurrences, if necessary.
- Q4. Ref. "Meyer-Abich 1956" is cited in the body but its bibliographic information is missing. Kindly provide its bibliographic information in the list.
- Q5. Please check if the edit to the sentence “We used a compact sensor unit containing...” retained the intended meaning.
- Q6. All occurrences of “tons/day” were changed to “t/day” for consistency. Please check if appropriate. Otherwise, please advise on how to proceed.
- Q7. Figure: Upon checking, it was noticed that there are panel labels in the caption of Figure 4; however, they were not found in the corresponding image. Please be informed that these were reflected in the image of the said figure to match their description in the figure caption. Please check if the action taken is appropriate. Otherwise, please advise on how to proceed.
- Q8. Please check if the table is presented correctly.
- Q9. Ref. "Battaglia et al. 2018" is cited in the body but its bibliographic information is missing. Kindly provide its bibliographic information in the list.
- Q10. Please check if the figure captions are captured and presented correctly.
- Q11. If applicable, please provide the access dates of references GVP (Global Volcanism Program), (2018) .